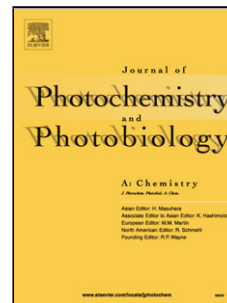


Accepted Manuscript

Title: Spacer Controlled Photo-Induced Intramolecular Electron Transfer in a Series of Phenothiazine-Boron Dipyrromethene Donor-Acceptor Dyads

Author: Naresh Duvva Kolanu Sudhakar Deepak Badgurjar
Raghu Chitta Lingamallu Giribabu



PII: S1010-6030(15)00263-4
DOI: <http://dx.doi.org/doi:10.1016/j.jphotochem.2015.07.007>
Reference: JPC 9964

To appear in: *Journal of Photochemistry and Photobiology A: Chemistry*

Received date: 18-5-2015
Revised date: 27-6-2015
Accepted date: 10-7-2015

Please cite this article as: Naresh Duvva, Kolanu Sudhakar, Deepak Badgurjar, Raghu Chitta, Lingamallu Giribabu, Spacer Controlled Photo-Induced Intramolecular Electron Transfer in a Series of Phenothiazine-Boron Dipyrromethene Donor-Acceptor Dyads, *Journal of Photochemistry and Photobiology A: Chemistry* <http://dx.doi.org/10.1016/j.jphotochem.2015.07.007>

This is a PDF file of an unedited manuscript that has been accepted for publication. As a service to our customers we are providing this early version of the manuscript. The manuscript will undergo copyediting, typesetting, and review of the resulting proof before it is published in its final form. Please note that during the production process errors may be discovered which could affect the content, and all legal disclaimers that apply to the journal pertain.

Spacer Controlled Photo-Induced Intramolecular Electron Transfer in a Series of Phenothiazine-Boron Dipyrromethene Donor-Acceptor Dyads

Naresh Duvva,^a Kolanu Sudhakar,^a Deepak Badgurjar,^b Raghu Chitta,^{b*} Lingamallu Giribabu^{a*}

^aInorganic & Physical Chemistry Division, CSIR-Indian Institute of Chemical Technology, Tarnaka, Hyderabad – 500007, Telangana, India. giribabu@iict.res.in.

^bSchool of Chemical Sciences & Pharmacy, Central University of Rajasthan, Bandarsindri, Tehsil: Kishangarh, Distt. Ajmer, Rajasthan – 305817, India. raghuchitta@curaj.ac.in.

Graphical abstract

Highlights

- A series of phenothiazine (PTZ)-boron dipyrromethene (BODIPY) based donor-acceptor dyads, tethered together with spacers of varied sizes are reported.
- Ground state properties indicates that there exist a moderate π - π interactions between PTZ and BODIPY units.
- Excited state properties indicates that there is an intramolecular photoinduced electron from ground state of PTZ to singlet state of BODIPY.
- The electron transfer rates (k_{ET}) of these dyads were found to be solvent dependent and were in the range 0.06×10^8 to $71.96 \times 10^{10} \text{ s}^{-1}$.

Abstract

A series of phenothiazine (PTZ)-boron dipyrromethene (BODIPY) based electron donor-acceptor dyads, **PB1**, **PB2**, and **PB3**, containing PTZ as an electron donor and BODIPY as an electron acceptor, tethered together with spacers of varied sizes i.e., directly connected (absence of the spacer), phenyl bridge, and ethoxy phenyl spacer, respectively, are reported. Optical absorption spectra of the dyads showed marginal ground state interactions between the chromophores and, these interactions are found more pronounced in **PB1** and **PB2**. Electrochemical studies on the dyads revealed minor shifts in the first oxidation of PTZ moiety and the first reduction of BODIPY moiety, compared to their control compounds. In the newly synthesized dyads, the free-energy calculations performed by employing the redox and singlet excited state energies, in both polar and non-polar solvents, suggested the possibility of electron transfer from the ground state of PTZ to the singlet excited BODIPY moiety (PTZ

→¹BODIPY*) to produce PTZ⁺-BODIPY⁻. Accordingly, steady state emission studies revealed the efficient fluorescence quenching of the singlet excited BODIPY in the dyads and the efficiency of quenching for all the dyads is higher in polar solvents. More importantly, these emission studies also revealed that, in a given solvent, as the length of the spacer between the chromophores is increased, the efficiency of fluorescence quenching is decreased. The degree of electronic communication between the chromophores w.r.t. the spacer type and size was supported by density functional theory (DFT) and time dependent-DFT (TD-DFT) calculations. The electron transfer rates (k_{ET}) of these dyads were found to be solvent dependent and were in the range 0.06×10^8 to $1.96 \times 10^{10} \text{ s}^{-1}$.

Key Words: BODIPY, Phenothiazine, Dyads, Intramolecular, Electron transfer, Spacer type and size, Time-resolved.

Corresponding authors: giribabu@iict.res.in, Phone: +91-40-27191724, Fax: +91-40-27160921; raghuchitta@curaj.ac.in, Phone: +91-1463-238535.

1. Introduction

Studies on photo-induced electron transfer (PET) events occurring in artificial donor-acceptor systems, that mimic the natural photosynthetic machinery, form as viable information to address the mechanistic details of electron transfer in chemistry and biology,[1,2] to develop artificial photosynthetic systems for harvesting solar energy[3-10] and, to build opto-electronic devices. [11] Several molecular and supramolecular dyads, triads, tetrads etc. have been elegantly designed and studied with an emphasis of generating long-lived charge separated states *via* charge migration route and achieved longer lifetimes for the charge separated states.[12-18] Systematic investigations exploring the role of photosensitizer (electron donor), nature of the electron acceptor, the spacer connecting the donor-acceptor entities, the spatial orientation of the donor-acceptor entities have provided a significant and valuable information necessary for the direct utilization of these systems for various light harvesting applications. In order to build these donor-acceptor systems, several porphyrins[19,20] or porphyrin like chromophores such as phthalocyanines,[21] sub-phthalocyanines,[22,23] corroles,[24] etc., and non-porphyrin like molecules, ferrocene,[25,26] triphenylamines,[27] phenothiazines[28,29] have been chosen as electron donors and quinones,[30] perylenediimides,[31] and fullerenes (C_{60} & C_{70})[32] have been utilized as electron acceptors. Among the electron acceptors, fullerene (C_{60}) has been extensively utilized, compared to any other acceptor, due to its remarkable electrochemical and optical properties and, more importantly, small re-organization energy in electron transfer reactions.[33]

Among the electron donors utilized for the purpose, unarguably, porphyrin or porphyrin like molecules have dominated the area of research as photoactive entity due to their resemblance to the natural photosynthetic chlorophyll pigment, rich photo- and electrochemical properties, and relatively easy synthetic modifications.[19,20] However, the tendency of porphyrins or porphyrin like molecules to form aggregates and participate in self-quenching, has limited the wide range of opto-electronic applications.[34] On the other hand, chromophores such as phenothiazines (PTZ) have gained attraction as suitable electron donors in donor-acceptor conjugates[28] and potential *p*-type material in organic devices[35] due to several interesting structural, photophysical and electrochemical properties. In general, PTZ derivatives absorb in the UV region, exhibit low oxidation potentials and possess a high propensity to form stable radical cations.[36,37] One of the most striking structural features of phenothiazine is that the ring is non-planar with a butterfly conformation in the ground state, which impedes the molecular aggregation and inhibit the formation of intermolecular aggregation and self-quenching.[38] Thus, because of its ground state intra-molecular charge transfer (ICT) and excited state PET, PTZs are regarded as excellent donors and widely used in making organic light emitting diodes,[39,40] acid-base dyes, and pigments[41] etc.

Towards the goal of constructing new artificial photosynthetic systems that possess the ability to convert light into chemical energy, BF₂-chelated dipyrromethene compounds, 4,4-difluoro-1,3,5,7-tetramethyl-4-bora-3a,4a-diaza-s-indacene (abbreviated as BODIPY) and its structural analogue, BF₂-chelated tetraarylazadipyrromethenes (aza-BODIPY), have attracted much attention in recent years as antenna molecules, electron donors and electron acceptors.[42] In particular, BODIPYs are versatile functional dyes with high stability and favourable photophysical and electrochemical properties, which can be tuned readily through chemical modification of the BODIPY core.[43] Generally, they exhibit large molar absorptivities ($\epsilon \approx 10^5 \text{ M}^{-1}\text{cm}^{-1}$), relatively high fluorescence quantum yields (0.57 in CH₂Cl₂), and relatively long singlet excited state lifetimes ($\approx 4\text{-}6 \text{ ns}$).[40] As a result, they have been extensively used as energy-absorbing and transferring antenna molecules in photosynthetic antenna-reaction center mimics,[44,45] and PET donor[46] and acceptor entities.[42,47]

Despite many reports of PTZ and BODIPY containing them separately are published in the literature, only a few cases, however, containing systems with BODIPY tethered to either one or two PTZ moieties and amalgamating the properties of both these chromophores have been reported. Some of these include, the photosynthetic antenna-

center mimic involving BODIPY as energy funnelling entity to porphyrazine and PTZ as a sacrificial electron donor,[47] chiral BODIPY and aza-BODIPY-based D- π -A conjugated polymers involving PTZ as electron donor,[48,49] Recently, D'Souza *et al* has reported PTZ-BODIPY-C₆₀ triads as photosynthetic reaction center models and studied the effect of solvents and the substitution on the photo-induced charge separation and recombination.[50] However, the study was limited to only two dyads i.e., PTZ connected to BODIPY either directly (no spacer) or via phenyl bridge and comprehensive photo-induced electron transfer studies w.r.t. the spacer size and type were not presented. In the present study, donor-spacer-acceptor systems involving BODIPY covalently connected to PTZ moieties, especially with systematic variation of spacers, and photo-induced electron transfer events w.r.t. the spacer type and sizes, in three different solvents (hexanes, CH₂Cl₂ and acetonitrile) is reported. Such kind of study is quite important to understand the variations in energetics of electron transfer w.r.t. the type and size of the spacer, and utilize these concepts in systematically controlling the electron transfer in various molecular and opto-electronic devices. To this, we have synthesized a series of PTZ-BODIPY based electron donor-acceptor systems, **PB1**, **PB2**, and **PB3**, tethered together with varied spacer types and sizes i.e., absence of spacer (directly connected), phenyl bridge, and saturated ethoxyphenyl spacer, respectively, and studied the effect of the spacer in photo-induced electron transfer events associated with these donor-acceptor conjugates. The molecular structures of the dyads and the control compounds are shown in Chart 1.

2. Experimental Section

2.1. Chemicals. Commercially available reagents and chemicals were procured from Sigma-Aldrich. Analytical reagent (AR) grade solvents were used for the reactions while laboratory reagent (LR) grade solvents were used for purifications and column chromatography. CH₂Cl₂, chloroform, acetonitrile and *N,N*-dimethylformamide were dried in presence of calcium hydride under nitrogen atmosphere. Hexanes were purified using sodium metal added benzophenone by refluxing overnight, distilled under vacuum and stored over 4Å molecular sieves. Triethylamine was distilled with NaOH pellets. ACME silica gel (100-200 mesh) was used for column chromatography. Thin-layer chromatography was performed on Merck-pre-coated silica gel 60-F254 plates. Either gravity or flash chromatography was performed for purification of all compounds. All the

reactions were carried out under nitrogen or argon atmosphere using dry and degassed solvents.

2.2. Synthetic procedure. *N,N'*-difluoroboryl-1, 3, 7, 9-tetramethyl-5-phenyldipyrrin (**BODIPY**),^[51] 10-(*n*-hexyl)-10*H*-phenothiazine (**1**),^[52] 10-(*n*-hexyl)-10*H*-phenothiazine-3-carbaldehyde (**2**)^[53] were synthesized according to the literature procedures.

2.2.1. 10-(4-Formylphenyl)phenothiazine (3): K₃PO₄ (0.53g, 2.5mmol) was added to a glass vial containing phenothiazine (0.1 g, 0.5 mmol) and the 4-fluorobenzaldehyde (0.12 g, 1 mmol), in dry DMF solvent (5 mL). The vial was sealed with a Teflon cap and the mixture was heated at 170°C for 48 hours. The mixture was cooled to room temperature and then poured into 200 mL of water and the product was extracted using methylene chloride. The organic layer was dried over anhydrous Na₂SO₄ and concentrated under reduced pressure to give the crude product. The crude product was purified by silica gel column chromatography and the desired compound was eluted with petroleum ether/ethylacetate (10:2, v/v) as light yellow colour solid. Yield: 0.12 g (79%). ¹H NMR (500 MHz, CDCl₃): δ (ppm) 9.75 (s, 1H, -CHO), 7.65 (d, J = 8.1 Hz, 2H, phenyl-aromatic *H*), 7.35 (d, J = 8.6 Hz, 2H, phenyl-aromatic *H*), 7.15-7.25 (m, 4H, phenothiazine-aromatic *H*), 7.0-7.10 (m, 4H, phenothiazine-aromatic *H*). MALDI-TOF: (*m/z*) found 304 (M⁺, C₁₉H₁₃NOS requires 303.38).

2.2.2. 10-(2-bromoethyl)-10H-phenothiazine (4): To a suspension of sodium hydride (60% mineral oil, 1.2 g, 50.2 mmol) in DMF was added a solution of phenothiazine (5g, 0.025 mol) in DMF and stirred at 0°C under nitrogen. After 30 min., the reaction mixture was heated to room temperature and stirred for 1h under nitrogen. Then the reaction mixture was cooled to 0°C, 1,2-dibromoethane (47 g, 0.25 mol) was added and the temperature was raised to 90°C and stirred for 12 h under nitrogen. After cooling, the reaction mixture was washed with water and extracted using ethyl acetate. The combined organic extracts were washed with brine solution, dried over Na₂SO₄ and filtered. The crude compound was purified using silica gel column chromatography and the desired compound was eluted using petroleum ether:ethylacetate (20:1, v/v). Evaporation of the solvent under the reduced pressure yielded the titled compound as a white solid. Yield: 3.8 g (49%). ¹H NMR (500 MHz, CDCl₃): δ (ppm) 7.11-7.07 (d, J = 8.0 Hz, 4H, phenothiazine-aromatic *H*), 6.91-6.86 (t, J = 10 Hz, 2H, phenothiazine-aromatic *H*), 6.80-6.76 (d, J = 12 Hz, 2H, phenothiazine-aromatic *H*), 4.22-4.17 (t, J = 10 Hz, 2H, Br-CH₂),

3.58-3.53 (t, $J = 9.4$ Hz, 2H, $N-CH_2$). MALDI-TOF: (m/z) found 306.11 (M^+ , $C_{14}H_{12}BrNS$ requires 306.22).

2.2.3. 4-(2-(10H-phenothiazin-10-yl)ethoxy)benzaldehyde (5): 4-hydroxybenzaldehyde (0.1 g, 0.8 mmol) was dissolved in DMF (50 mL) and dry potassium carbonate (0.9 g, 6.5 mmol) was added and stirred under nitrogen for 30 min. Then **4** (0.5g, 1.6 mmol) was added and the reaction mixture was stirred at 90°C for 3 h. Then the reaction mixture was cooled and the solvent was evaporated. Water was added and the mixture was extracted using ethyl acetate. Evaporation of the organic extracts yielded the crude compound which was purified by silica gel column chromatography using petroleum ether/ethylacetate (20:1, v/v) as an eluent. Evaporation of the solvent yielded the titled compound as light yellow solid. Yield: 0.4g (71%). 1H NMR (500 MHz, $CDCl_3$): δ (ppm) 9.88 (s, 1H, -CHO), 7.83-7.80 (d, $J = 8.8$ Hz, 2H, phenyl-aromatic H), 7.18-7.16 (d, $J = 8.2$ Hz, 4H, phenyl-aromatic $2H$ & phenothiazine-aromatic $2H$), 7.00-6.93 (m, 6H, phenothiazine-aromatic H), 4.38 (4H, s, $O-CH_2$ & $N-CH_2$). MALDI-TOF: (m/z) found 348.02 (M^+ , $C_{21}H_{17}NO_2S$ requires 347.43).

2.2.4. Synthesis of Dyads: 2,4-dimethylpyrrole (0.64 g, 6.72 mmol) and corresponding aldehyde (3.36 mmol) were dissolved in absolute CH_2Cl_2 (200 mL) (*nitrogen gas was bubbled through CH_2Cl_2 for 30 min.*) under N_2 atmosphere. One drop of trifluoroacetic acid (TFA) was added and the solution was stirred at room temperature for 2 h. At this point, a solution of 2,3-dichloro-5,6-dicyano-1,4-benzoquinone (DDQ) (0.77 g, 3.36 mmol) in 50 mL absolute CH_2Cl_2 was added, stirred for 1h followed by the addition of Et_3N (4.5 mL, 3.4 g, 33.62 mmol) and $BF_3 \cdot OEt_2$ (3.4 mL, 3.8 g, 26.9 mmol). After 30 min., the reaction mixture was extracted with CH_2Cl_2 and the organic layer was dried over anhydrous Na_2SO_4 . Evaporation of the solvent under reduced pressure gave the crude product, which upon purification by silica gel column chromatography using dichloromethane/hexane (1:1 v/v) as eluent gave the corresponding dyad.

N,N' -difluoroboryl-1,3,7,9-tetramethyl-5-[10-(n -hexyl)-10H-phenothiazin-3-yl]dipyrrin (PB1): Yield: 310 mg (18%). 1H NMR (500MHz, $CDCl_3$): δ (ppm) 7.19-7.16 (m, 1H, phenothiazine-aromatic H), 7.11-7.09 (dd, $J = 7.6$ Hz 1.5 Hz, 1H, phenothiazine-aromatic H), 7.01-6.99 (dd, $J = 7.4$ Hz 1.5 Hz, 2H, phenothiazine-aromatic H), 6.95-6.87 (m, 3H, phenothiazine-aromatic H), 5.97 (s, 2H, pyrrole H), 3.89-3.86 (t, $J = 7.3$ Hz, 2H, $N-CH_2$), 2.54 (s, 6H, pyrrole- CH_3), 1.85-1.79 (m, 2H, aliphatic H), 1.51 (s, 6H, pyrrole- CH_3), 1.47-1.41 (m, 2H, aliphatic H), 1.38-1.34 (m, 2H, aliphatic H), 1.32-1.28(m, 2H,

aliphatic *H*), 0.89-0.85(t, *J* = 7.1 Hz, 3H, aliphatic *H*).MALDI-TOF: (*m/z*) found 530 (M^+ , $C_{31}H_{34}BF_2N_3S$ requires 529.49).

N,N'-difluoroboryl-1,3,7,9-tetramethyl-5-[4-(10H-phenothiazin-10-

yl)phenyl]dipyrrin (PB2): Yield: 0.36 mg (30%). 1H NMR (500 MHz, $CDCl_3$): δ (ppm) 7.51 (s, 4H, phenyl-aromatic *H*), 7.11-7.09 (dd, *J* = 7.8 Hz 1.3 Hz, 2H, phenothiazine-aromatic *H*), 6.92- 6.88 (m, 4H, phenothiazine-aromatic *H*), 6.38-6.36 (dd, *J* = 7.9 Hz 1.6 Hz, 2H, phenothiazine-aromatic *H*), 6.04 (s, 2H, pyrrole-*H*), 2.58 (s, 6H, pyrrole- CH_3), 1.56 (s, 6H, pyrrole- CH_3). MALDI-TOF: (*m/z*) found 521.88 (M^+ , $C_{31}H_{26}BF_2N_3S$ requires 521.43).

N,N'-difluoroboryl-1,3,7,9-tetramethyl-5-[4-(2-(10H-phenothiazin-10-

yl)ethoxy)phenyl]dipyrrin (PB3): Yield: 0.21g (26%). 1H NMR (500 MHz, $CDCl_3$): 7.18-7.13 (m, 6H, phenyl-aromatic 4*H*& phenothiazine-aromatic 2*H*), 7.01-6.96 (dd, *J* = 7.4 Hz 1.2 Hz, 6H, phenothiazine-aromatic *H*), 5.97 (s, 2H, pyrrole-*H*), 4.37 (s, 4H, *O-CH_2*&*N-CH_2*), 2.54(s, 6H, pyrrole- CH_3), 1.41 (s, 6H, pyrrole- CH_3). MALDI-TOF: (*m/z*) found 566.02 (M^+ , $C_{33}H_{30}BF_2N_3OS$ requires 565.48).

2.3. Methods and Instrumentation.

2.3.1. Characterization: 1H -NMR spectra were recorded on a 500MHz INOVA spectrometer. Cyclic and differential pulse voltammograms (DPV) measurements were performed on a PC-controlled electrochemical analyzer (CH instruments model CHI620C). All the experiments were performed with 1 mM concentration of compounds in CH_2Cl_2 at a scan rate of 100 mVs^{-1} in which tetrabutylammoniumperchlorate (TBAP) is used as a supporting electrolyte as documented in our previous reports.[54,55]

2.3.2. Absorption and fluorescence measurements: The optical absorption spectra were recorded on a Shimadzu (Model UV-3600) spectrophotometer. Concentrations of solutions are ca. to be 1×10^{-6} M. Steady-state fluorescence spectra were recorded on a Fluorolog-3 spectrofluorometer (Spex model, JobinYvon) for solutions with optical density at the wavelength of excitation (λ_{ex}) ≈ 0.1 . Fluorescence quantum yields (ϕ) were estimated by integrating the fluorescence bands and by using N,N'-difluoroboryl-1,3,7,9-tetramethyl-5-(4-carboxy)phenyldipyrrin (BODIPY- CO_2H)[56] ($\phi = 0.57$ in CH_2Cl_2), when excited at 503 nm. Phenothiazine (PTZ) compounds were almost non-fluorescent, when excited at λ_{ex} 254 nm.[57] Fluorescence lifetime measurements were carried on a picosecond time-correlated single photon counting (TCSPC) setup (FluoroLog3-Triple

Illuminator, IBH Horiba JobinYvon) employing a picosecond light emitting diode laser (NanoLED, $\lambda_{\text{ex}}=470$ nm) as excitation source. The decay curves were recorded by monitoring the fluorescence emission maxima of the dyads ($\lambda_{\text{em}}=500$ nm). Photomultiplier tube (R928P, Hamamatsu) was employed as the detector. The lamp profile was recorded by placing a scatterer (dilute solution of Ludox in water) in place of the sample. The width of the instrument function was limited by the full width at half maxima (FWHM) of the excitation source, ~ 625 ps at 405 nm. Decay curves were analyzed by nonlinear least-squares iteration procedure using IBH DAS6 (version 2.3) decay analysis software. The quality of the fits was judged by the χ^2 values and distribution of the residuals.

2.3.3. Theoretical calculations: Full geometry optimization of the dyads **PB1**, **PB2**, and **PB3** were carried out by Gaussian 09 (Revision B.01) *ab initio* quantum chemical software[58] in the personal computer. Density Functional Theory (DFT) was used to determine the ground state properties, while time dependent-DFT (TD-DFT) was employed for estimation of ground state to excited state transitions. B3LYP method[59] and 6-31G (d,p) basis set[60] were used to optimize the geometries of the dyads to be genuine global minimum energy structures. The geometries were used to obtain the frontier molecular orbitals (FMOs) and were also subjected to single-point TD-DFT studies (First 15 vertical singlet–singlet transitions) to obtain the UV-Vis spectra of the dyes. The integral equation formalism polarizable continuum model (PCM)[61] within the self-consistent reaction field (SCRF) theory was used in the TDDFT calculations to describe the solvation of the dyes in CH_2Cl_2 . The software GaussSum 2.2.5 was employed to simulate the major portions of the absorption spectra and to interpret the nature of transitions.[62] The contribution percentages of individual units present in the dyes to the respective molecular orbitals were calculated.

3. Results and Discussion

3.1. Syntheses of Phenothiazine-BODIPY dyads. The methodology developed for the synthesis of phenothiazine functionalized BODIPY dyes, **PB1**, **PB2** and **PB3**, with varied spacers is shown in Scheme 1, while the details of the syntheses are given in the Experimental Section. The phenothiazine moieties bearing aldehyde functional groups, **2**, **3** and **5**, required for the synthesis of BODIPYs are synthesized in one or two steps using slightly modified literature procedures. Briefly, N-(n-hexyl)-phenothiazine, **1** was formylated at the 3-position by standard Vilsmeier-Haack formylation procedure[51] by

the reaction of **1** with POCl_3 in DMF to yield 10-(n-hexyl)-10H-phenothiazine-3-carbaldehyde, **2** while the one-pot reaction of 4-fluorobenzaldehyde with pristine phenothiazine in presence of K_3PO_4 at high temperatures in DMF produced 10-(4-formylphenyl)phenothiazine, **3** in good yields. However, 4-(2-(10H-phenothiazin-10-yl)ethoxy)benzaldehyde, **5** was synthesized by reacting phenothiazine with 1,2-dibromoethane in DMF in the presence of NaH to obtain **4** followed by its reaction with 4-hydroxybenzaldehyde in presence to K_2CO_3 in DMF. Phenothiazine functionalized BODIPY dyes **PB1**, **PB2**, and **PB3**, were synthesized by a one-pot reaction involving the condensation of the corresponding aldehyde with 2,4-dimethylpyrrole in presence of trifluoroacetic acid to make dipyrromethane substituted at the *meso*-position w.r.t. phenothiazine entity. Subsequent treatment of these dipyrromethanes with DDQ, triethylamine, BF_3 -etherate afforded the crude compounds as a black reaction mixture. Evaporation of the solvent and purification of these crude products by silica gel column chromatography afforded the target molecules as orange crystals.[51] The newly synthesized compounds have been fully characterized by mass, ^1H NMR and other spectroscopic techniques. ^1H NMR, MALDI-TOF mass spectra of the precursors and the final compounds are shown in the supporting information Figures S1-S12. For example, The peak at m/z 212.29 corresponds to “10-methyl-10H-phenothiazine”. The peak at m/z 1131 might correspond to the dyad of **PB3**.

3.2. Optical Absorption Studies. Figure 1 show the optical absorption spectra of the investigated compounds along with pristine **PTZ** and **BODIPY** used as the control compounds. Spectroscopic data which include wavelength of maximum absorbance (λ_{max}), molar extinction coefficients ($\log \epsilon$) of the dyads and the control compounds are summarized in Table 1. The control compound, **PTZ** revealed two distinct peaks at 254 and 316 nm in dichloromethane which were assigned to the localized aromatic $\pi-\pi^*$ transitions.[63] The reference compound, **BODIPY** exhibited three minor intense absorption bands at 227 nm and between 305-400 nm, and a major intense absorption band at 501 nm corresponding to the electronic transition from the ground state to the first excited state (S_0-S_1 transition). Tethering the phenothiazine moieties to BODIPY chromophores did not reveal any drastic spectral changes except minor spectral changes in the UV and visible region. Compared to pristine **PTZ**, the phenothiazine moiety in the dyads **PB1**, **PB2**, and **PB3** having the substitution on the aromatic ring or on hetero atom revealed the spectra with a split band in the UV region at 227-240 nm and 245-285

nm ranges.[57] This spectral change may be attributed to the loss of symmetry in the phenothiazine frame work due to the introduction of **BODIPY** moiety. On the other hand, in case of all the dyads, the absorption peaks between 300 – 400 nm are blue shifted (~5 – 9 nm) compared to the control compounds, **PTZ** and **BODIPY**, displaying very marginal ground state interactions within the chromophores in these dyads. Also, in case of **PB1** and **PB2**, the characteristic peak at 503 nm corresponding to the **BODIPY** moiety is red shifted ~2 nm, compared to the control compound **BODIPY** ($\lambda_{\text{max}} = 501$ nm), while similar changes are not observed in case of **PB3**. This marginal shift may be attributed to the better electronic communication between the two chromophores, **PTZ** and **BODIPY** moieties, in the dyads (*vide infra*).

Such kind of weak ground state interactions generated between energy/electron donors and acceptors that are tethered together have been reported earlier.[16,45] However, under these conditions, it was difficult to isolate any weak band corresponding to charge-transfer type interactions between **PTZ** and **BODIPY** moieties. More importantly, the stronger absorption of **BODIPY** between 425–530 nm ($\lambda_{\text{max}} = 501$ nm) has no overlap with the **PTZ** absorption in this wavelength range indicating that irradiation of the dyad at 485 nm would selectively excite the **BODIPY** moiety of the dyad.

3.3. Electrochemical Studies. The electrochemical behaviour of the dyads was investigated using cyclic and differential pulse voltammetric techniques. Figure 2 illustrates the differential pulse voltammograms of **PB1**, **PB2**, and **PB3**, and Table 2 summaries the redox potential data (CH_2Cl_2 and 0.1 M TBAP) of the donor-acceptor systems investigated in this study along with the control compounds. Figure 2 and Table 2 indicate that the dyads investigated showed two oxidation and one reduction peaks under the experimental conditions employed for the study. Wave analysis suggested that, in general, the first two oxidation steps and the one reduction step are reversible ($i_{\text{pc}}/i_{\text{pa}} = 0.9-1.0$) and diffusion controlled ($i_{\text{pc}}/v^{1/2} = \text{constant}$ in the scan rate (v) range 50-100 mVs^{-1}) one electron ($\Delta E_p = 60-70$ mV; $\Delta E_p = 65 \pm 3$ mV for ferrocenium/ferrocene couple) reactions. In contrast, in case of pristine **PTZ** molecule, we have observed quasi-reversible oxidation process.

All the dyads exhibited two one-electron oxidation peaks, with the first oxidation peak in the range of 0.76 – 0.80 V (**PB1**: 0.80 V; **PB2**: 0.77 V; **PB3**: 0.76 V) and a second oxidation peak in the range of 1.18 – 1.25 V (**PB1**: 1.18 V; **PB2**: 1.22 V; **PB3**: 1.25 V) under the employed experimental conditions. The first peak was due to the oxidation of

the **PTZ** moiety of the dyad ($\text{PTZ}^{\bullet+} - \text{BODIPY}$). The origin of the second oxidation peak was difficult to be assigned to a particular chromophore because the second oxidation of **PTZ** ($\text{PTZ}^{\bullet+}/2^+$: 1.18 V vs SCE) and the first oxidation of **BODIPY** (1.22 V vs SCE) in the control compounds were displayed at almost the same anodic potential. It should be noted here that, in case of all the dyads, the first oxidation peak is shifted ~ 170 mV towards higher anodic potentials compared to the first oxidation of pristine **PTZ** and this shift may be ascribed to the introduction of electron withdrawing entity, **BODIPY**, in the dyad which makes the **PTZ** hard to get oxidized compared to the pristine **PTZ**. However, the similar trend is not quite pronounced in case of the second oxidation potential of the dyads.

The dyads **PB1**, **PB2**, and **PB3** undergo single one-electron reversible reduction at -1.16 V, -1.08 V, and -1.18 V respectively. The origin of this peak is due to the reduction of the **BODIPY** moiety of the dyad ($\text{PTZ} - \text{BODIPY}^{\bullet-}$). In case of these dyads, it was observed that the reduction peak was shifted ~ 160 mV towards lower reduction potentials compared to the control compound, **BODIPY**, centered at -1.24 V. This cathodic shift may be ascribed to the introduction of electron donating entity, **PTZ**, in the dyad which makes the **BODIPY** easy to reduce compared to the control compound.

The driving forces for charge separation (ΔG_{CS}) in three different solvents of varying polarity, hexanes, CH_2Cl_2 and acetonitrile, were evaluated using the Weller-type approach[64,65] utilizing the redox potentials, center-to-center distance ($R_{\text{c-c}}$), dielectric constant of the solvents and the E_{0-0} values and listed in the Table 3. Generation of the charge separated state ($\text{PTZ}^{\bullet+} - \text{BODIPY}^{\bullet-}$) was exothermic via the singlet excited states of the **BODIPY** in all the three solvents and followed the trend acetonitrile $>$ CH_2Cl_2 $>$ hexanes for a given dyad (*vide infra*). It should be mentioned here that no apparent shifts in the redox potentials w.r.t. the variation in the spacer type or sizes between **PTZ** and **BODIPY** moieties was observed in these dyads. Cyclic voltammograms of the dyads and the controlled compounds are shown in the supporting information S13.

In order to further assign the redox potentials of these dyads, we have carried our spectroelectrochemical studies. Figure 3 indicates *in-situ* spectral changes of **PB3** in dichloromethane solvent during the applied potential. When applied potential at 0.90V, the absorption band at 254 nm (absorption belongs to pristine **PTZ**) reduces its intensity with formation of new at 270 nm and finally it disappears with an isosbestic point at 265

nm (Figure 3a). In contrast the absorption bands at 233 and 500 nm (absorption belongs to pristine BODIPY) remain unchanged. This clearly suggest the oxidation at 0.76 V belongs to PTZ moiety. Spectroscopic changes during the controlled potential application at -1.30 V are shown in Figure 3b. The absorption band at 500 nm reduces with intensity with the formation of isosbestic points at 260, 360 and 465 nm.[66] Whereas the absorption bands at UV regions remains unchanged. This clearly suggestion the reduction potential at -1.18 is belongs to BODIPY moiety. Similar spectral changes were also observed in case of **PB1** and **PB2** dyads.

3.4. Computational Studies. To visualize the geometry, electronic structure and optical properties of the dyads, computational studies were performed at the DFT and TD-DFT studies using B3LYP/6-31G(d,p) level.[60] For this, the dyads were optimized on a Born-Oppenheimer potential energy surface, and a global minimum for each dyad was obtained. The energy-optimized structures and the molecular electrostatic potential (MEP) maps for the dyads, **PB1** and **PB2**, are shown in Figure 4a & b, while for the dyad, **PB3**, is shown in Figure S15a & b in the supporting information. For all the investigated dyads, it is observed that the **PTZ** moiety, in its neutral state, is bent around the N-S axis with an angle of $\sim 147.1^\circ$, which is in agreement with the value reported in the literature.[67] The edge-to-edge (R_{e-e}) and center-to-center distances (R_{c-c}) between the **PTZ** and **BODIPY** moieties in the dyads were estimated and summarized in Table 4. In the MEP maps, for all the dyads, the positive electrostatic potential was at the phenothiazine and spacer connecting the chromophores, while the negative potential was concentrated at the pyrrolic -NH and -BF₂ groups of **BODIPY**. Frontier highest occupied molecular orbital (HOMO) and lowest unoccupied molecular orbital (LUMO) for the dyads, **PB1** and **PB2** are shown in Figure 4c, & d. In case of **PB1**, the HOMO was located on the **PTZ** and **BODIPY** π -system, suggesting strong interaction between the donor and acceptor entities, while the LUMO was located on the **BODIPY** moiety. In **PB2**, the HOMO was located on the PTZ moiety while the LUMO on the **BODIPY** moiety. Importantly, parts of the HOMO and LUMO were also located on the phenyl spacer, suggesting a notable interaction between donor and acceptor entities in **PB2**. However, it should be noted from the electronic distribution of frontier orbitals that the interaction between donor and acceptor is weaker in case of **PB2** as compared to **PB1**. The locations of the HOMO and LUMO also suggested the formation of the charge-separated state (PTZ^{•+} - BODIPY^{•-}) due to photoinduced electron transfer process.

In the case of dyad **PB3**, an increased donor-acceptor distance and less spreading of the frontier orbitals were observed (see Figure S15c-f in the Supporting Information). In contrast to the above dyads, in **PB3**, the HOMO and LUMO are located on the BODIPY moiety, while the HOMO-1 and LUMO+1 are located on the PTZ moiety. This may be attributed to very low energy difference between HOMO and HOMO-1 in this dyad. However, the electrochemical studies revealed that **PTZ** moiety is oxidized at a lower potential than BODIPY and, hence, as seen in case of **PB1**, **PB2**, and **PB3**, it can be expected that PTZ moiety would act as electron donor and **BODIPY** moiety as the electron acceptor. The calculated gas phase HOMO–LUMO gap was found to be in the range of 2.99 eV and 2.65 eV for the dyads.

Based on the experimental observations, TD-DFT studies of these molecules were carried using B3LYP energy functional with the 6-31G (d,p) basis set in order to gain a deeper understanding of the excited-state transitions with the framework of the polarizable continuum model (PCM) in CH₂Cl₂ as the solvent. These results are in reasonable agreement with the experimental values. The singlet state properties of maximum wavelength absorbance, oscillation strength (f), excited state energy (E) in eV and the percentage contribution of molecular orbital of all three dyads by means of absorption spectra are presented in Supporting Information. Theoretical absorption spectra of **PB1**, **PB2**, and **PB3**, (see in supporting information (Fig. S16) of each dyad segment has been computed from the frontier molecular orbitals by using the GaussSum software.

3.5. Fluorescence Emission Studies. The photochemical behaviour of the phenothiazine-BODIPY dyads was investigated, using steady-state fluorescence measurements. As can be seen in Figure 5a-c, the emission spectra of all the three dyads, **PB1**, **PB2**, and **PB3**, along with their reference compound, **BODIPY**, were measured in hexanes, CH₂Cl₂, and acetonitrile solvents by exciting them at $\lambda = 485$ nm, wavelength at which **BODIPY** moiety absorbs, and corresponding wavelengths of emission maxima and quantum yields are presented in Table 5. Attempts to record the emission of the dyads and reference compound **PTZ** by exciting the **PTZ** moiety at $\lambda_{\text{max}} = 254$ nm, did not yield any noticeable emission in case of the dyads and yielded very low intensity peak for pristine **PTZ** (see Figure S14 in the Supporting information).[57] Hence, in the present discussion, all the dyads were excited at $\lambda = 485$ nm and the resultant emission changes are presented. It should be mentioned here that, in order to ensure that the **BODIPY**

moiety is selectively excited at this wavelength ($\lambda_{\text{ex}} = 485 \text{ nm}$), excitation spectra of all the dyads in three solvents were recorded by monitoring the emission at 510 nm corresponding to **BODIPY** and compared with their absorption spectra (see Figure S17 in the Supporting Information). By overlapping both the spectra, it was found that the excitation spectra of the dyads did not show any characteristic peaks pertaining to **PTZ** and hence, it was confirmed that the **BODIPY** moiety was predominantly excited at this wavelength. The emission of all the dyads was quenched when equi-absorbing solutions of dyads, in three solvents, were excited at $\lambda_{\text{ex}} = 485 \text{ nm}$, where **BODIPY** moiety absorbs predominantly. The possibility of self-aggregation of the chromophores, either **BODIPY** or **PTZ** in a dyad, which may lead to fluorescence quenching, can be ruled out as all the experiments were performed in very dilute solutions (10^{-6} M). For the dyads, the quenching efficiency was found in the range of $\sim 3\%$ to 39% in hexanes, 71% to 99% in CH_2Cl_2 and 84% to 99% in acetonitrile. The quenching efficiency is more in case of **PB1** (no spacer directly connected) and **PB2** (phenyl bridge) compared to **PB3** (ethoxy phenyl spacer).

Various radiative and non-radiative intramolecular processes can be responsible for the excited state decay of the dyads. Among these, an excitation energy transfer (EET) or photo-induced electron transfer (PET) can be conceived in the quenching of fluorescence emission intensity. For EET to occur, the emission spectrum of the energy donor should be well matched with the absorption spectrum of the acceptor. It is evident from Figure 1 & 4 that, as the emission of **BODIPY** ($\lambda_{\text{em}} = 512 \text{ nm}$) does not overlap with the absorption of **PTZ** moiety ($\lambda_{\text{abs}} = 260 \text{ nm}$ & 310 nm), the possibility of EET from $^1\text{BODIPY}^*$ moiety to **PTZ** can be eliminated. Also, as **PTZ** is very weakly emissive (see Figure S14 in the Supporting Information) and there is no apparent emission in the region where **BODIPY** absorbs (*vide supra*), the possibility of EET from $^1\text{PTZ}^*$ to **BODIPY** can also be eliminated. Hence, no experiments demonstrating this phenomenon are performed in this report. Alternative pathway for emission quenching is the intramolecular PET from the ground state of phenothiazine moiety to the singlet state of **BODIPY** to produce $\text{PTZ}^{\bullet+}\text{-BODIPY}^{\bullet-}$. However, it should be mentioned here that the $^1\text{BODIPY}^*$ produced by excitation could undergo inter system crossing (ISC) to populate $^3\text{BODIPY}^*$ ($\sim 1.76 \text{ eV}$),[54] alternatively it could undergo electron transfer to produce $\text{PTZ}^{\bullet+}\text{-BODIPY}^{\bullet-}$. [50] E_{0-0} , energy due to 0-0 electronic transition, of **BODIPY** moiety of dyads was found to be $\sim 2.44 \text{ eV}$ (estimated from intersecting wavelength of the

absorption and emission spectra of BODIPY) for all the dyads, which is comparable to E_{0-0} value of control compound **BODIPY**. The change in the free energy due to PET from the ground state of phenothiazine to the singlet excited **BODIPY** moiety can be calculated by using the Eq. (1).

$$\Delta G_{CS}(\text{PTZ} \rightarrow {}^1\text{BODIPY}^*) = E_{CT}(\text{PTZ}^+-\text{BODIPY}^{\bullet-}) - E_{0-0}(\text{BODIPY}) - X \quad (1)$$

Where the term X accounts for the finite donor-acceptor separation (R_{C-C}), ionic radii (r^+ , r^-) and solvent dielectric constant (ϵ_s),

$$X = \frac{e^2}{4\pi\epsilon_0\epsilon_s R_C} + \frac{e^2}{8\pi\epsilon_0} \left(\frac{1}{r^+} + \frac{1}{r^-} \right) \left(\frac{1}{\epsilon_{ref}} - \frac{1}{\epsilon_s} \right) \quad (2)$$

$\text{PTZ}^+-\text{BODIPY}^{\bullet-}$ is the difference in the oxidation and reduction potentials of PTZ and BODIPY moieties of the dyads in three solvents. The radii of the molecular ions used were $r^+ = 3.623 \text{ \AA}$ and $r^- = 3.372 \text{ \AA}$ from computational calculations. The centre-to-centre distance for the dyads **PB1**, **PB2**, and **PB3** were found to be 7.256 \AA , 8.771 \AA , and 12.001 \AA respectively, from energy minimization studies (Table 4). The driving forces for charge separation (ΔG_{CS}) were found to be exothermic (negative) in the solvents, hexanes, CH_2Cl_2 , and acetonitrile, for all the dyads when excited at 485 nm. The solvent polarity dependent negative ΔG indicates that there is a possibility of PET from PTZ to ${}^1\text{BODIPY}^*$.

Fluorescence quantum yields of the dyads and the individual components in the three solvents, have been estimated (Table 5) by comparing the emission curves of reference compound (i.e., BODIPY, $\Phi_f = 0.98 \pm 0.01\%$ in CH_2Cl_2) with those of the dyads. It was found that the fluorescence quantum yield (Φ_f) of **PB1**, **PB2**, and **PB3** were found to be 0.01, 0.01, and 0.289 respectively in CH_2Cl_2 . The fluorescence emission quenching efficiency of the dyads was calculated using Eq. (3).

$$\%Q = \frac{\Phi(\text{BODIPY}) - \Phi(\text{dyad})}{\Phi(\text{BODIPY})} \quad (3)$$

Where $\Phi(\text{BODIPY})$ and $\Phi(\text{dyads})$ refer to the fluorescence quantum yields of control compound **BODIPY** and the dyads, respectively, when excited at $\lambda_{ex} = 485 \text{ nm}$.

In addition, the evidence of the PET process of these D-A systems was obtained from the excited state fluorescence decay measurements. Any excited state non-radiative process would be expected to decrease fluorescence emission intensity and thereby fluorescence lifetime. Figure 6 represents excited state decay curves **PB1**, **PB2** & **PB3** in

CH₂Cl₂ solvent and corresponding decay parameters are collected in Table 6. From the data, it is clear that the fluorescence lifetimes, τ ($\lambda_{\text{ex}} = 485$ nm and $\lambda_{\text{em}} = \sim 510$ nm) of the dyads are decreased in all the solvents when compared to the reference compound **BODIPY**.^[68] All dyads except in hexane solvent, decay curves are fitted with a bi-exponential expression: shorter lifetime component is attributed to the deactivation (quenching) of the excited **BODIPY** by phenothiazine. Minor longer lifetime component perhaps might be due to the unquenched decay of **BODIPY** unit of dyad or different conformers that included face-to-face originated from donor-acceptor-donor type of molecular arrangement. Also, as the length of the spacer increases, as in case of **PB3**, closed and extended conformers may be possible, which may be responsible for the minor longer lifetime component.^[69]

Further, rate constant (k_{ET}) for the charge transfer state $\text{PTZ}^{*+}\text{--BODIPY}^{*-}$ have been calculated using eq. (3) and summarized in Table 3.

$$k_{\text{ET}} = (1/\tau_{\text{f}}) - k \quad (3)$$

Where k is the reciprocal of the lifetime of the **BODIPY**, τ_{f} is the lifetime of dyads in respective solvent. The solvent-dependent k_{ET} values are in the range of $0.71 \times 10^8 \text{ s}^{-1}$ to $1.96 \times 10^{10} \text{ s}^{-1}$ for **PB2** and $0.06 \times 10^8 \text{ s}^{-1}$ to $1.81 \times 10^9 \text{ s}^{-1}$ for **PB3**. The observed general increase of the k_{ET} values with increasing polarity of the solvent is consistent with the participation of a charge transfer state in the excited state deactivation of **BODIPY** component of these D-A system. On the basis of these calculations, an energy level diagram involving the photo-induced electron transfer events can be depicted for all the dyads. For example, an energy level diagram depicting the photochemical events in all the solvents for dyad **PB2** is shown in Figure 7. Similar diagrams for the dyads **PB1** and **PB3** are shown in the Figure S18a & b in the Supporting information.

3.5.1. Effect of solvent polarity on PET. As the static dielectric constant of the solvent was increased, quenching of the fluorescence intensity was increased (see Figure 4). In other words, with increasing the polarity of the solvent, a gradual decrease in the fluorescence quantum yield was observed (Table 5), which further demonstrates the excited state electron transfer mechanism. In addition to this the excited state decay also follows polarity of the solvent. For a particular dyad, the quenching efficiencies are less in hexanes compared to CH₂Cl₂ and acetonitrile and followed the trend hexanes < CH₂Cl₂ < acetonitrile. These results are in good agreement with the literature information that, as

the charge separated state ($\text{PTZ}^{*+} - \text{BODIPY}^{*-}$) is relatively more stabilized in the polar solvents, the PET process is accelerated in polar medium rather than non-polar medium.[70]

3.5.2. Effect of spacers on PET. In addition to the effect of solvent polarity on PET processes, the effect of proximity of **PTZ** and **BODIPY** moieties in the dyads on PET events was also studied using the steady state fluorescence studies. In detail, it was observed that, for a particular solvent, as the length of the spacer between **PTZ** and **BODIPY** moieties is increased i.e., no spacer (directly connected) in **PB1**, phenyl bridge in **PB2** and saturated ethoxy phenyl spacer in **PB3**, the efficiency of fluorescence quenching is decreased and followed the order **PB1**>**PB2**>**PB3**. For example, in hexanes, the efficiency of PET and hence, fluorescence quenching is high for **PB1** (39%) compared to **PB2** (8%) and **PB3** (3%). Similar results were also observed for the dyads in CH_2Cl_2 and acetonitrile. This can be attributed to a fact that the efficiency of PET depends on the overlap of the electron clouds between the donor and acceptor moieties.[71] In **PB1**, as **PTZ** (donor) and **BODIPY** (acceptor in excited state) moieties are directly connected i.e., no spacer, the overlap of the electron clouds and the electronic communication between **PTZ** and **BODIPY** is expected to be more (see section 3.4.) and, thus, the fluorescence quenching efficiency is high compared to other dyads in all the three solvents. Similarly, in case of **PB2** and **PB3**, as the length of the spacer is increased, the degree of electronic communication between the **PTZ** and **BODIPY** may be decreased which resulted in the lower fluorescence quantum efficiency in the solvents investigated. Hence, from the above discussion it can be concluded that these dyads enabled us to control the efficiency of PET w.r.t. different spacers and served as excellent models to study the effect of type and size of the spacer on the PET events.

Conclusions

This work presents a series of electron donor-acceptor systems, **PB1**, **PB2**, and **PB3**, consisting of phenothiazine as an electron donor and **BODIPY** as an acceptor that are connected via spacers of different types and sizes. All the dyads were synthesized and characterized using various spectroscopic and electrochemical methods. Optical absorption studies showed marginal interactions between the chromophores in the ground state, while the electrochemical studies have revealed minor shifts in the redox potentials, probably, due to tethering of electron donating **PTZ** moiety to an electron withdrawing **BODIPY** moiety. DFT and TD-DFT studies using B3LYP/6-31G(d,p) calculations

showed stronger electronic communication in **PB1** compared to **PB2** and **PB3** in the ground level as well as excited level. Similar effects were observed in the steady state and time resolved fluorescence studies revealing that, upon photo-excitation of **BODIPY**, an intramolecular PET was occurred from the ground state **PTZ** to **¹BODIPY*** generating **PTZ^{•+}-BODIPY^{•-}**. More interestingly, the extent of quenching is greater for **PB1** and **PB2** *i.e.*, in the dyads containing donor and acceptor at a relatively closer distance compared to **PB3** and the quenching was more efficient in polar solvents compared to non-polar solvents.

Acknowledgements

We are grateful to Department of Science and Technology (DST, SB/S1/IC-14/2014) and Central University of Rajasthan for financial support of this work. The authors ND and DB acknowledges Council of Scientific and Industrial Research (CSIR) for Junior Research Fellowship (JRF) and Central University of Rajasthan for Research Fellowship respectively.

References

1. R. A. Marcus, Electron transfer reactions in chemistry: theory and experiment. *Angew. Chem. Int. Ed. Engl.* 32 (1993) 1111-1121.
2. C. Kirmaier, D. Holton. In the photosynthetic reaction center, J. Deisenhofer, J. R. Norris, Eds.; Academic Press: San Diego, 1993; Vol. II, pp 49-70.
3. M.M.A. Keloson, R.S. Bhosale, K. Ohkubo, L.A. Jones, S.V. Bhosale, A. Gupta, S. Fukuzumi, S.V. Bhosale, A simple zinc porphyrin-NDI dyad system generates a light energy to proton potential across a lipid membrane. *Dye and Pigments* 120 (2015) 340-346.
4. L.-B. Meng, D. Li, S. Xiong, X.-Y. Hu, L. Wang, G. Li, FRET capable supramolecular polymers based on a BODIPY-bridged pillar[5]arene dimer with BODIPY guests for mimicking the light-harvesting system of natural photosynthesis. *Chem. Commun.* 51 (2015) 4643-4646.
5. S. Fukuzumi, S.; Ohkubo, K.; Suenobu, T. Long-lived charge separation and applications in artificial photosynthesis. *Acc. Chem. Res.* 47 (2014) 1455-1464.
6. H. -J. Xu, A. Bonnot, P. -L. Karsenti, A. Langlois, M. Abdelhameed, J. -M. Barbe, C. -P. Gros, P. D. Harvey, Antenna effects in truxene-bridged BODIPY triarylzinc(II) porphyrin dyads: evidence for a dual Dexter-Forster mechanism. *Dalton Trans.* 43 (2014) 8219 – 8229.
7. P. K. Poddutoori, N. Zarrabi, A. G. Moiseev, R. Gumbau-Brisa, S. Vassiliev, A. vanderEst, Long-lived charge separation in novel axial donor-porphyrin-acceptor triads based on

- tetrathiafulvalene, aluminum(III) porphyrin and naphthalenediimide. *Chem. Eur. J.* 19 (2013) 3148-3161.
8. B. Grimm, J. Schornbaum, H. Jasch, O. Trukhina, F. Wessendorf, A. Hirsch, T. Torres, D. M. Guldi, Step-by-Step self-assembled hybrids that future control over energy and charge transfer. *PNAS* 109 (2012) 15565-15571.
 9. G. D. Scholes, G. R. Flemming, A. Olaya-Castro, R. vanGrondelle, Lessons from nature about solar light harvesting. *Nature Chem.* 3 (2011) 763-774.
 10. R. Chitta, F. D'Souza, Self-assembled tetrapyrrole–fullerene and tetrapyrrole–carbon nanotube donor–acceptor hybrids for light induced electron transfer applications. *J. Mater. Chem.* 18 (2008) 1440-1471.
 11. J. J. Bergkamp, S. Decurtins, S. X. Liu, Current advances in fused tetrathiafulvalene donor-acceptor systems. *Chem. Soc. Rev.*, 44 (2015) 863-874.
 12. M. Gilbert, Photoinduced charge and energy transfer in molecular wires. *Chem. Soc. Rev.*, 44 (2015) 845-862.
 13. L. Giribabu, J. Kandhadi, R. K. Kanaparthi, Phosphorus(V) corrole-porphyrin based hetero trimers: synthesis, spectroscopy and photochemistry. *J. Fluoresc.* 24 (2014) 569-577.
 14. L. Giribabu, P. S. Reeta, R. K. Kanaparthi, M. Srikanth, Y. Soujanya, Bis(Porphyrin)-anthraquinone triads: synthesis, spectroscopy and photochemistry. *J. Phys. Chem. A* 117 (2013) 2944-2951.
 15. M. Marszalek, S. Naqane, A. Ichake, R. Humphry-Baker, V. Paul, S. M. Zakeeruddin, M. Gratzel, Tuning spectral properties of phenothiazine based donor– π –acceptor dyes for efficient dye-sensitized solar cells. *J. Mater. Chem.* 22 (2012) 889-894.
 16. F. D'Souza, R. Chitta, K. Ohkubo, M. Tasior, N. K. Subbaiyan, M. E. Zandler, M. K. Rogacki, D. T. Gryko, S. Fukuzumi, Corrole-fullerene dyads: formation of long-lived charge-separated states in non-polar solvents. *J. Am. Chem. Soc.* 130 (2008) 14263-14272.
 17. X. -H. Zhang, S. H. Kim, I. S. Lee, Ch. J. Gao, S. I. Yang, K. -H. Ahn, Synthesis, photophysical and electrochemical properties of novel conjugated donor-acceptor molecules based on phenothiazine and benzimidazole. *Bull. Korean Chem. Soc.* 28 (2007) 1389-1395.
 18. B. Schlicke, L. De Cola, P. Belser, V. Balzani, Rigid rod-like molecular wires of nanometric dimension. electronic energy transfer from a naphthyl to an anthracenyl unit connected by a 1,4-pentaphenylene spacer. *Coord. Chem. Rev.* 208 (2000) 267–275.

19. D. Gust, T. A. Moore, A. L. Moore, Solar fuel via artificial photosynthesis. *Acc. Chem. Res.* 42 (2009) 1890-1898.
20. F. D'Souza, O. Ito, Photoinduced electron transfer in supramolecular systems of fullerenes functionalized with ligands capable of binding to zinc porphyrin and zinc phthalocyanines. *Coord. Chem. Rev.* 249 (2005) 1410-1422.
21. J. Kandhadi, R. K. Kanaparthi, L. Giribabu, Germanium(IV) phthalocyanine-porphyrin based hetero trimers: synthesis, spectroscopy and photochemistry. *J. Porphyrins & Phthalocyanines* 16 (2012) 282-289.
22. D. González-Rodríguez, C. G. Claessens, T. Torres, S. G. Liu, L. Echegoyen, N. Vila, S. Nonell, Tuning photoinduced energy- and electron-transfer events in subphthalocyanine–phthalocyanine dyads. *Chem.-Eur. J.* 11 (2005) 3881–3893.
23. D. González-Rodríguez, T. Torres, D. M. Guldi, J. Rivera, M. A'. Herranz, L. Echegoyen, Subphthalocyanines: tuneable molecular scaffolds for Intramolecular Electron and Energy Transfer Processes. *J. Am. Chem. Soc.* 126 (2004) 6301–6313.
24. L. Giribabu, K. Sudhakar G. Sabapathi, R. K. Kanaparthi, Intramolecular photoinduced reactions in corrole-pyrene and corrole-fluorene dyads. *J. Photochem. Photobiol. A Chem.* 284 (2014) 18-26.
25. S. Gokulnath, B. S. Achary, Ch. K. Kumar, R. Trivedi, B. Sreedhar, L. Giribabu, Synthesis, structure and photophysical properties of ferrocenyl or mixed sandwich cobaltocenyl ester linked meso-tetratolylporphyrin dyads. *Photochem. Photobiol.* 91 (2015) 33-41.
26. A. N. Amin, M. E. El-Khouly, N. K. Subbaiyan, M. E. Zandler, M. Supur, S. Fukuzumi, F. D'Souza, Syntheses, electrochemistry, and photodynamics of ferrocene–azadipyrrromethane donor–acceptor dyads and triads. *J. Phys. Chem. A.* 115 (2011) 9810-9819.
27. L. Giribabu, K. Sudhakar, Photoinduced intramolecular reactions in triphenylamine–corrole dyads. *J. Photochem. Photobiol. A Chem.* 196 (2015) 11-18.
28. S.-H. Lee, C. T. Chan, K. M. Wong, W. H. Lam, W. Kwok, V. W. Yam, Design and synthesis of bipyridine platinum(II) bisalkynyl fullerene donor–chromophore–acceptor triads with ultrafast charge separation. *J. Am. Chem. Soc.* 136 (2014) 10041-10052.
29. C. B. KC, G. N. Lim, M. E. Zandler, Synthesis and photoinduced electron transfer studies of a tri(Phenothiazine)–subphthalocyanine–fullerene pentad. *Org. Lett.* 15 (2013) 4612-4615.

30. R. Jono, K. J. Yamashita, Two different lifetimes of charge separated states: a porphyrin–quinone system in artificial photosynthesis. *J. Phys. Chem. C* 116 (2012) 1445-1449.
31. J. Wenzel, A. Dreuw, I. Burghardt, Charge and energy transfer in a bithiophene perylenediimide based donor-acceptor system for use in organic photovoltaics. *PhysChemChemPhys*. 28 (2013) 11704-11716.
32. M. E. El-Khouly, O. Ito, P. M. Smith, F. D'Souza, Intermolecular and supramolecular photoinduced electron transfer processes of fullerene–porphyrin/phthalocyanine systems. *J. Photochem. Photobiol. C: Photochem. Rev.* 5 (2004) 79-104.
33. M. J. Prato, [60]Fullerene chemistry for material science applications. *J. Mater. Chem.* 7 (1997) 1097-1109.
34. L. Giribabu, R. K. Kanaparthi, Are porphyrins are alternative to ruthenium(II) sensitizers for dye-sensitized solar cells. *Current Sci.* 104 (2013) 847-855.
35. G. Marotta, M. A Reddy, S. P. Singh, A. Islam, L. Han, F. D. Angelis, M. Pastore, M. Chandrasekharam, Novel carbazole-phenothiazine dyads for dye-sensitized solar cells: a combined experimental and theoretical study. *ACS Appl. Mater. Interfaces* 5 (2013) 9635-9647.
36. T. -S. Hsieh, J. -Y. Wu, C. -C. Chang, Multiple fluorescent behaviors of phenothiazine-based organic molecules. *Dyes Pigments* 112 (2015) 34-41.
37. M. In. Sainsbury, M. R. Sainsbury, *Rodd's chemistry of carbon compounds*. 2nd Ed., 4. Amsterdam: Elsevier; 1998, pp575-608.
38. C. S. Kramer, K. Zeitler, T. J. Müller, Synthesis of functionalized ethynylphenothiazine fluorophores. *Org. Lett.* 2 (2000) 3723-3726.
39. M. Sailer, A. W. Franz, T. J. Muller, Synthesis and electronic properties of monodisperse oligophenothiazines. *Chem.-Eur. J.* 14 (2008) 2602-2614.
40. G. W. Kim, M. J. Cho, Y. J. Yu, Z. H. Kim, J. I. Jin, D. Y. Kim, Red emitting phenothiazine dendrimers encapsulated 2-{2-[2-(4- dimethylaminophenyl)vinyl]-6-methylpyran-4-ylidene}malonitrile derivatives. *Chem. Mater.* 19 (2007) 42-50.
41. R. R. Gupta, *Phenothiazines and 1,4-benzothiazines – chemical and biomedical Aspects*, Chapter 2. Amsterdam; Elsevier; 1988.
42. M. E. El-Khouly, S. Fukuzumi, F. D'Souza, Photosynthetic antenna–reaction center mimicry by using boron dipyrromethene sensitizers. *ChemPhysChem* 15 (2014) 30-47 (references therein).
43. A. Loudet, K. Burgess, *BODIPY Dyes and their derivatives: syntheses and spectroscopic properties*. *Chem. Rev.* 107 (2007) 4891-4932.

44. Y. Terazono, G. Kodis, P. A. Liddell, T. A. Moore, A. L. Moore, D. Gust, Multiantenna artificial photosynthetic reaction center complex. *J. Phys. Chem. B* 113 (2009) 7147-7155.
45. F. D'Souza, P. M. Smith, M. E. Zandler, A. L. McCarty, M. Itou, Y. Araki, O. Ito, Energy transfer followed by electron transfer in a supramolecular triad composed of boron dipyrin, zinc porphyrin, and fullerene: a model for the photosynthetic antenna-reaction center complex. *J. Am. Chem. Soc.* 126 (2004) 7898-7907.
46. D. Frath, J. E. Yarnell, G. Ulrich, F. N. Castellano, R. Ziessel, Ultrafast photoinduced electron transfer in viologen-linked BODIPY dyes. *ChemPhysChem* 14 (2013) 3348-3354.
47. V. Bandi, K. Ohkubo, S. Fukuzumi, F. D'Souza, A broad band capturing and emitting molecular triad: synthesis and photochemistry. *Chem. Commun.* 49 (2013) 2867-2869.
48. V. Engelhardt, S. Kuhri, J. Fleischhauer, M. García-Iglesias, D. González-Rodríguez, G. Bottari, T. Torres, D. M. Guldi, R. Faust, Light-harvesting with panchromatically absorbing BODIPY-porphyrazine conjugates to power electron transfer in supramolecular donor-acceptor ensembles. *Chem. Sci.* 4 (2013) 3888-3893.
49. X. Ma, E. A. Azeem, X. Liu, Y. Cheng, C. Zhu, Synthesis and tunable chiroptical properties of chiral BODIPY-based D- π -A conjugated polymers. *J. Mater. Chem. C* 2 (2014) 1076-1084.
50. C.B. KC, G. N. Lim, V. N. Nestrerov, P. A. Karr, F. D'Souza, Phenothiazine-BODIPY-fullerene triads as photosynthetic reaction center models: substitution and solvent polarity effects on photoinduced charge separation and recombination. *Chem. Eur. J.* 20 (2014) 17100-17112.
51. M. Kollmannsberger, K. Rurack, U. Resch-Genger, J. Daub, Ultrafast charge transfer in amino-substituted boron dipyrromethene dyes and its inhibition by cation complexation: a new design concept for highly sensitive fluorescent probes. *J. Phys. Chem. A* 102 (1998) 10211-10220.
52. X. Kong, A. P. Kulkarni, S. A. Jenekhe, Phenothiazine-based conjugated polymers: synthesis, electrochemistry, and light-emitting properties. *Macromolecules* 36 (2003) 8992-8999.
53. C.-J. Yang, Y. J. Chang, M. Watanabe, Y.-S. Hon, T. J. Chow, Phenothiazine derivatives as organic sensitizers for highly efficient dye-sensitized solar cells. *J. Mater. Chem.* 22 (2012) 4040-4049.

54. L. Giribabu, C. V. Kumar, V. G. Reddy, P. Y. Reddy, Ch. S. Rao, S. -R. Jang, J. -H. Yum, M. K. Nazeeruddin, M. Gratzel, Unsymmetrical alkoxy zinc phthalocyanine for sensitization of nanocrystalline TiO₂ films, *Sol. Energy Mater. Sol. Cells* 91 (2007) 1611-1617.
55. L. Giribabu, C. V. Kumar, P. Y. Reddy, Porphyrin-rhodanine dyads for dye sensitized solar cells. *J. Porphyrins&Phthalocyanines* 10 (2006) 1007-1016.
56. C. Aijun, P. Xiaojun, F. Jiangli, C. Xiuying, W. Yunkou, G. Binchen, Synthesis, spectral properties and photostability of novel boron-dipyrromethene dyes. *J. Photochemistry and Photobiology A: Chemistry* 186 (2007) 85–92.
57. A. S. Hart, K. C. Bikram, N. K. Subbaiyan, P. A. Karr, F. D'Souza, Phenothiazine-sensitized organic solar cells: effect of dye anchor group positioning on the cell performance. *ACS Appl. Mater. Interfaces* 4 (2012) 5813-5820.
58. M. J. Frisch, G. W. Trucks, H. B. Schlegel, G. E. Scuseria, M. A. Robb, J. R. Cheeseman, G. Scalmani, V. Barone, B. Mennucci, G. A. Petersson, H. Nakatsuji, M. Caricato, X. Li,; H. P. Hratchian, A. F. Izmaylov, J. Bloino, G. Zheng, J. L. Sonnenberg, M. Hada, M. Ehara, K. Toyota, R. Fukuda, J. Hasegawa, M. Ishida, T. Nakajima, Y. Honda, O. Kitao, H. Nakai, T. Vreven, J. A. Montgomery Jr, J. E. Peralta, F. Ogliaro, M. Bearpark,; J. J. Heyd, E. Brothers, K. N. Kudin, V. N. Staroverov, R. Kobayashi, J. Normand, K. Raghavachari, A. Rendell, J. C. Burant, S. S. Iyengar, J. Tomasi, M. Cossi, N. Rega, N. J. Millam, M. Klene, J. E. Knox, J. B. Cross, V. Bakken, C. Adamo, J. Jaramillo, R. Gomperts, R. E. Stratmann, O. Yazyev, A. J. Austin, R. Cammi, C. Pomelli, J. W. Ochterski, R. L. Martin, K. Morokuma, V. G. Zakrzewski, G. A. Voth, P. Salvador, J. J. Dannenberg, S. Dapprich, A. D. Daniels, O. Farkas, J. B. Foresman, J. V. Ortiz, J. Cioslowski and D. J. Fox, *Gaussian 09, Revision B.01*, Gaussian, Inc., Wallingford CT, 2010.
59. A. D. Becke. A new mixing of hartree-fock and local density-functional theories. *J. Chem. Phys.* 98 (1993) 1372.
60. G. A. Petersson, M. A. Al-Laham. A complete basis set model chemistry II. open-shell systems and the total energies of the first-row atoms. *J. Chem. Phys.* 94 (1991) 6081.
61. M. Cossi, V. Barone, R. Cammi and J. Tomasi, Ab Initio study of solvated molecules: A new implementation of the polarizable continuum model, *Chem. Phys. Lett.*, 255 (1996) 327-335.
62. N. M. O'Boyle, A. L. Tenderholt and K. M. Langner, cclib: A library for package-independent computational chemistry algorithms, *J. Comput. Chem.* 29 (2008) 839-845.

63. M. L. Pascu, A. Smarandache, M. Boni, J. Kristiansen, V. Nastasa, I. R. Andrei, Spectral properties of some molecular solutions. *Rom. Rep. Phys.* 63 (2011) 1267-1284.
64. D. Rehm, A. Weller, Kinetics of fluorescence quenching by electron and H-atom transfer *Isr. J. Chem.* 7 (1970) 259-271.
65. N. Mataga, H. Miyasaka, In *Electron Transfer*; J. Jortner, M. Bixon, Eds.; John Wiley & Sons: New York, 1999; Part 2, pp 431-496.
66. O. Galagau, I. Fare-Francke, S. Munteanu, C. Dumas-Verdes, G. Clavier, R. Meallet-Renault, R. B. Pansu, F. Hartl, F. Miomandre, Electronic and electrofluorochromic properties of a new boron dipyrromethane-ferrocene conjugate. *Electrochim. Acta* 87 (2013) 809-815.
67. A. Monti, H. J. M. de Groot, F. Buda, In silico design of a donor-antenna-acceptor supramolecular complex for photoinduced charge separation. *J. Phys. Chem. C* 118 (2014) 15600-15609.
68. In case of **PB1**, unquenched excited state life-time was observed as the bond between **PTZ** and **BODIPY** was dissociated when exposed to laser for longer time. However, this was not observed in case of **PB2** and **PB3**.
69. F. D'Souza, R. Chitta, S. Gadde, D.M.S. Islam, A.L. Schumacher, M.E. Zandler, Y. Araki, O. Ito, Design and studies on supramolecular ferrocene-porphyrin-fullerene constructs for generating long-lived charge separated states. *J. Phys. Chem. B* 110 (2006) 25240-25250.
70. J. R. Bolton, J. A. Schmidt, T. F. Ho, J.-Y. Liu, K. R. Roach, A. C. Weedon, M. D. Archer, J. H. Wilford, V. P. Y. Gadzekpo, *Electron transfer in inorganic, organic and biological systems*, American Chemical Society, Chapter 7, 1991.
71. G. J. Kavarnos, *Fundamentals of photoinduced electron transfer*, VCH Publishers, Inc., 1993, Chapter 1, page 45.

Table 1: Absorption Data

$^a\lambda_{\max}$, nm (log ϵ , M ⁻¹ cm ⁻¹)						
Compound	Phenothiazine moiety			BODIPY moiety		
PTZ		254 (4.77)		316 (2.78)		
BODIPY	227 (4.49)			320 (3.78)	363 (3.76)	501 (5.14)
PB1	232 (4.72)	260 (4.96)		309 (4.38)		503 (5.23)
PB2	234	253 (5.82)	258 (5.00)	310 (4.36)	412 (4.34)	503 (5.14)
PB3	235 (4.73)	256 (4.72)		307 (3.95)	354 (3.96)	501 (5.07)

^aSolvent CH₂Cl₂, Error limits: λ_{\max} , ± 1 nm, log ϵ , $\pm 10\%$

Table 2: Electrochemical Data

Compound	Potential V vs. SCE ^a		
	Oxidation		Reduction
PTZ	0.63	1.18	-0.82
BODIPY		1.22	-0.94, -1.24
PB1	0.80	1.25	-1.16
PB2	0.77	1.22	-1.08
PB3	0.76	1.18	-1.18

^aCH₂Cl₂, 0.1 M TBAP; Glassy carbon working electrode, Standard calomel electrode is reference electrode, Pt electrode is counter electrode. Error limits, E_{1/2}±0.03 V

Table 3: First oxidation and reduction potentials (*E*, V vs SCE) and free-energy changes for charge-separation (ΔG_{CS}) for the dyads in hexanes, CH₂Cl₂ and acetonitrile.

Compound ^a	<i>E</i> (PTZ ^{0/+}) ^b /V	<i>E</i> (BODIPY ^{0/-})/V	- $\Delta G_{CS}(\text{PTZ-}^1\text{BODIPY}^*)^c/\text{eV}$		
			Hexanes	CH ₂ Cl ₂	Acetonitrile
PB1	0.80	-1.16	-0.451	-0.488	-0.507
PB2	0.77	-1.08	-0.554	-0.596	-0.614
PB3	0.76	-1.18	-0.464	-0.514	-0.531

^aSee Chart 1 for structures. ^bRedox potentials were obtained from DPV recorded in CH₂Cl₂.

^c $\Delta G_{CS} = (E_{ox} - E_{red}) - E_{0-0} - X$ where, *E*_{ox} and *E*_{red} are the one-electron oxidation and reduction potentials of phenothiazine and BODIPY moieties respectively,

$$X = \frac{e^2}{4\pi\epsilon_0\epsilon_S R_{ct-ct}} + \frac{e^2}{8\pi\epsilon_0} \left(\frac{1}{r^+} + \frac{1}{r^-} \right) \left(\frac{1}{\epsilon_{ref}} - \frac{1}{\epsilon_S} \right)$$

Where ϵ_0 , ϵ_S refers to vacuum permittivity and dielectric constant of the solvent, *R*_{ct-ct} is the donor-acceptor center-to-center distance, and *r*⁺ and *r*⁻ are the ionic radii (PTZ⁺ = 3.623 Å and BODIPY⁻ = 3.372 Å), *E*₀₋₀ is the energy of the lowest excited states (2.45 eV for ¹BODIPY* in CH₂Cl₂).

Table 4: B3LYP/6-31G (d,p)-Optimized Distances between PTZ and BODIPY moieties and related orbital energies in the investigated dyads.

Dyads	edge-to-edge distance, Å	center-to-center distance (R_{ct-ct}), Å	HOMO-1, eV	HOMO, eV	LUMO, eV	LUMO+1, eV
PB1	1.494	7.256	-5.332	-5.28	-2.291	-0.6533
PB2	5.744	8.771	-5.747	-5.133	-2.487	-0.9981
PB3	9.004	12.001	-5.354	-5.293	-2.294	-0.5260

Table 5: Fluorescence Data^a

Compound	λ_{em} , nm (Φ_f , % Q)		
	Hexanes	CH ₂ Cl ₂	Acetonitrile
PTZ ^b	-	-	-
BODIPY	512 (0.875)	512 (0.980)	509 (0.814)
PB1	514 (0.532, 39.2)	514 (0.010, 98.9)	509 (0.008, 99.0)
PB2	514 (0.803, 8.2)	514 (0.010, 98.9)	510 (0.010, 98.6)
PB3	512 (0.848, 3.1)	512 (0.289, 70.5)	509 (0.133, 83.5)

^aSpectra were measured at 293 ± 3 K. Error limits: λ_{em} , ± 1 nm; Φ_f , ± 10%; ^b λ_{ex} at 254 nm.

Table 6: Fluorescence Decay Parameter^a and electron transfer rate constants (k_{ET} , s⁻¹)^b

Compound	τ , ns (A, %), k_{ET} , s ⁻¹		
	Hexanes	CH ₂ Cl ₂	CH ₃ CN
BODIPY	2.74	3.26	3.18
PB1	3.00	3.01(40) 4.89(60)	2.24(20) 4.73(80)
PB2	2.29 0.71 x 10⁸	0.07(56) ^c 3.30(43) 1.39 x 10¹⁰	0.05(53) ^c 3.18(46) 1.96 x 10¹⁰
PB3	2.69 0.06 x 10⁸	0.86 (85) 1.96 (15) 8.56 x 10⁸	0.47(88) ^c 3.36(12) 1.81 x 10⁹

^aAll life times are in nanoseconds (ns), at $\lambda_{ex} = 485$ nm. ^bError limit of τ and k_{ET} , ~10%. Values in parenthesis are relative amplitude of corresponding decay component. ^cShort lifetime components are limited by the instrument response function (IRF).

Figure Captions:

Chart 1. Molecular structures of dyads **PB1**, **PB2**, **PB3**, and control compounds, **PTZ** and **BODIPY**.

Scheme 1. Synthetic route for the preparation of phenothiazine-BODIPY dyads and control compound, **BODIPY**, employed for the study.

Figure 1. Absorption spectra of the indicated compounds in CH₂Cl₂ at RT.

Figure 2. Differential pulse voltammograms (a) oxidation (b) reduction of the indicated compounds in CH₂Cl₂ containing 0.1 M (*n*-C₄H₉)₄NClO₄. The concentrations of the dyads were held at 1 mM; scan rate = 100 mVs⁻¹.

Figure 3. In-situ UV-Visible absorption changes of **PB3** at an applied potential of (a) 0.90 V (b) -1.30 V.

Figure 4. B3LYP/6-31G(d,p)-calculated (a) optimized structure, (b) molecular electrostatic potential map, (c) frontier LUMO, and (d) frontier HOMO of the dyads **PB1** and **PB2**. The red and blue colours in (b) indicate the negative and positive potentials.

Figure 5. Fluorescence spectra ($\lambda_{\text{ex}} = 485 \text{ nm}$) and ($\text{OD } \lambda_{\text{ex}} = 0.1$) of equi-absorbing solutions of **PB1** (black), **PB2** (red), **PB3** (green) and **BODIPY** (magenta) in (a) hexanes, (b) CH_2Cl_2 , and (c) acetonitrile.

Figure 6. Fluorescence decay curves of **BODIPY**, **PB1**, **PB2**, and **PB3** ($\lambda_{\text{ex}} = 470 \text{ nm}$, $\lambda_{\text{em}} = \sim 510 \text{ nm}$) in hexane, CH_2Cl_2 and acetonitrile.

Figure 7. Energy level diagram depicting the photochemical events in non-polar and polar solvents for the PTZ-BODIPY dyad **PB2**.

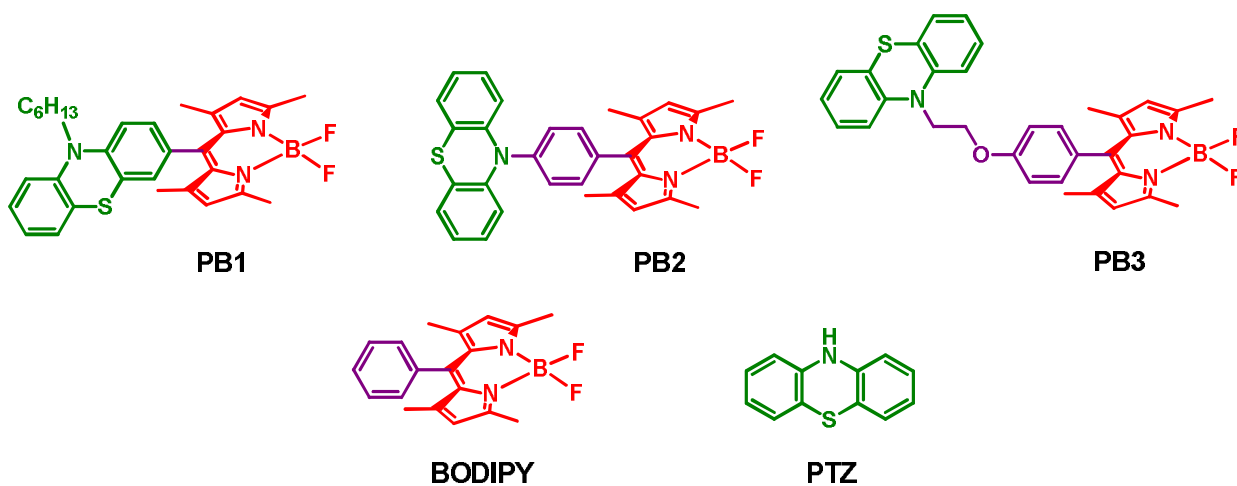
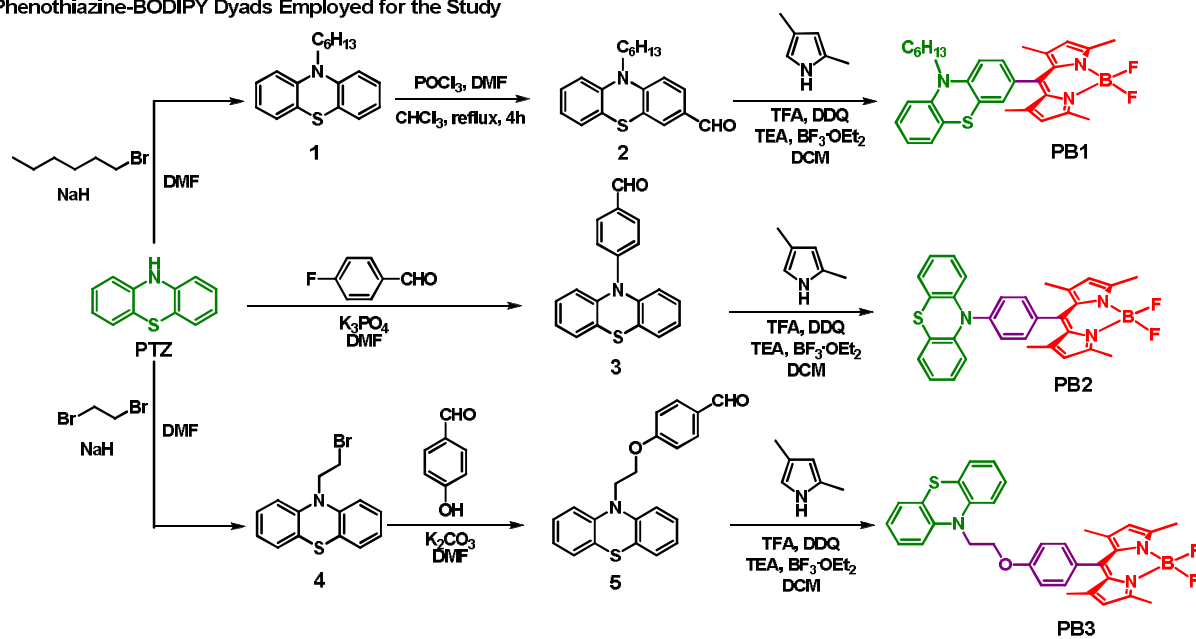
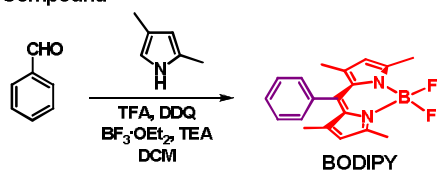


Chart1

(a) Phenothiazine-BODIPY Dyads Employed for the Study



(b) Control Compound



Scheme 1

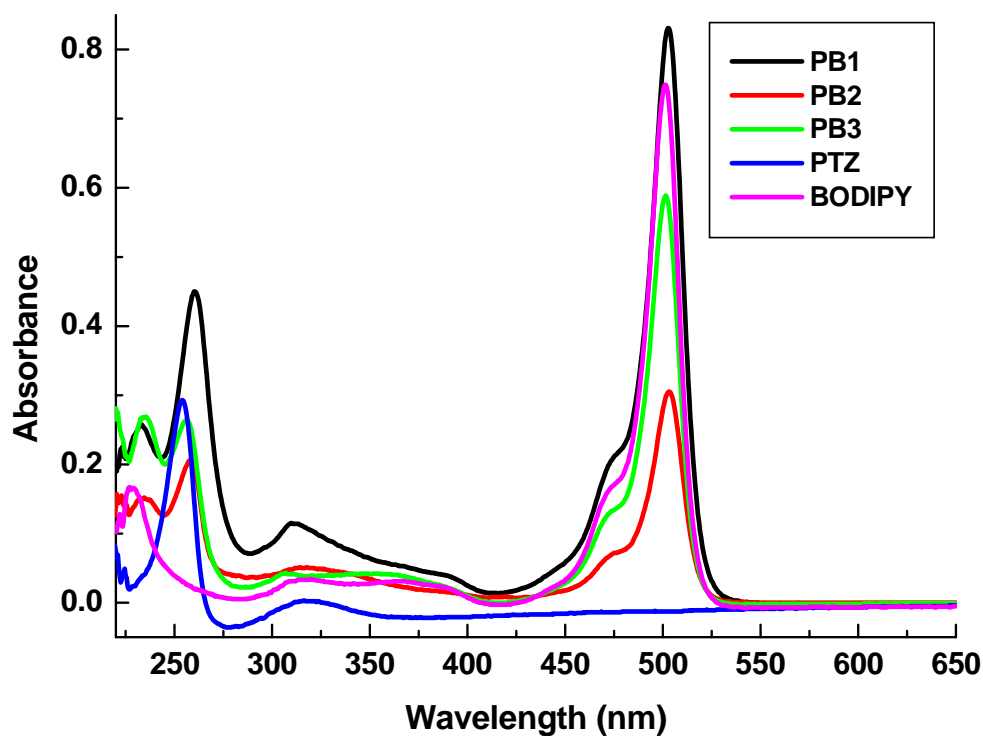


Figure 1

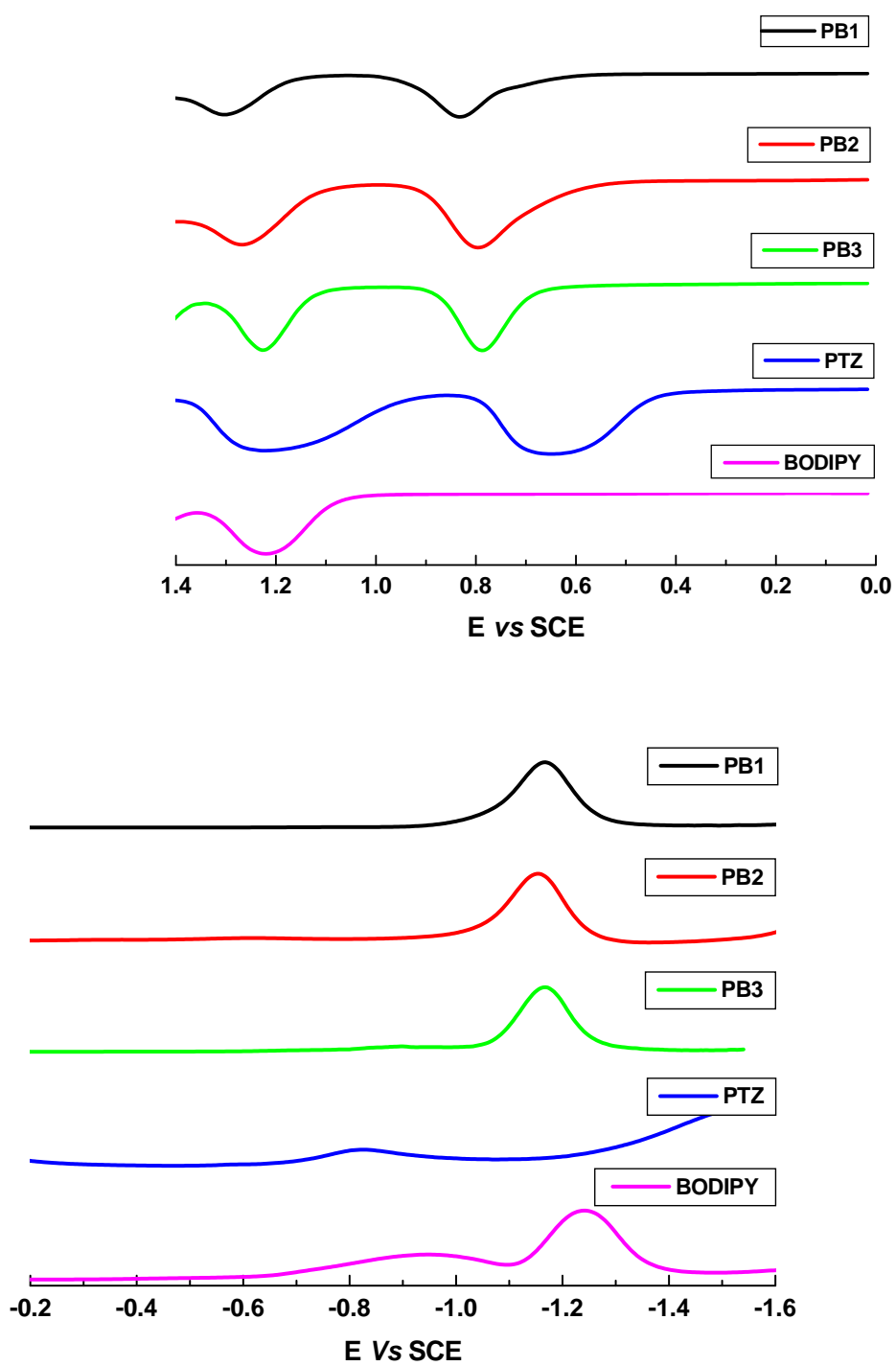
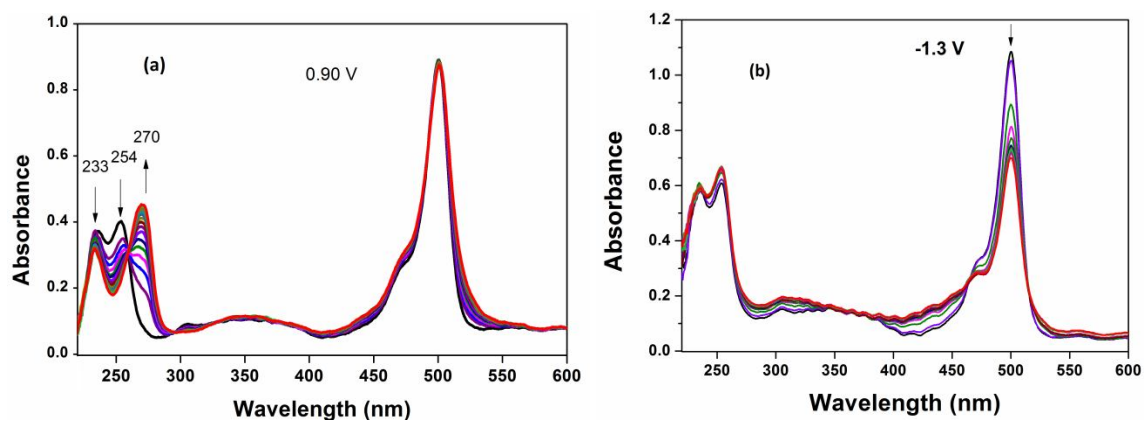


Figure 2



PB1

PB2

Figure 3

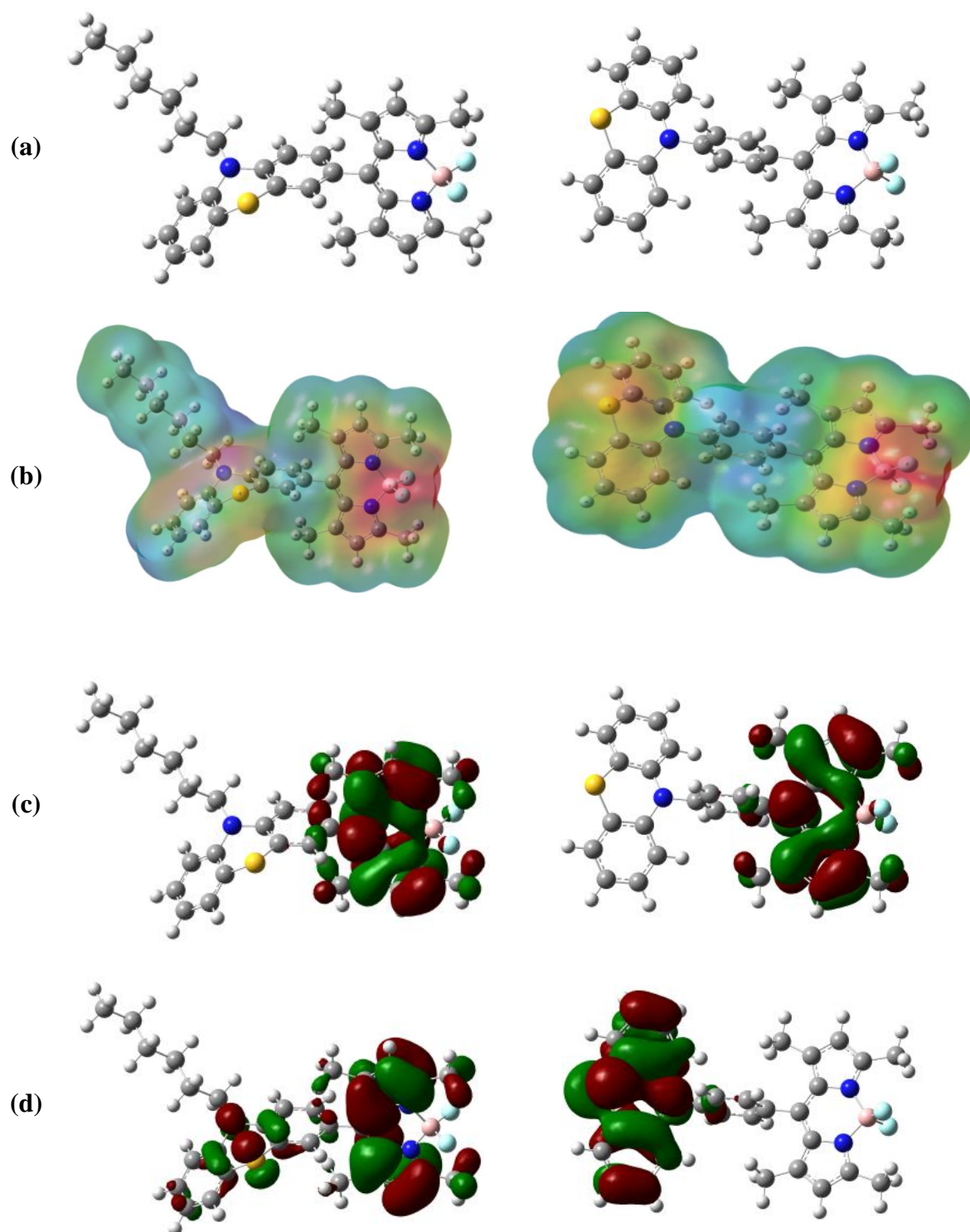


Figure 4

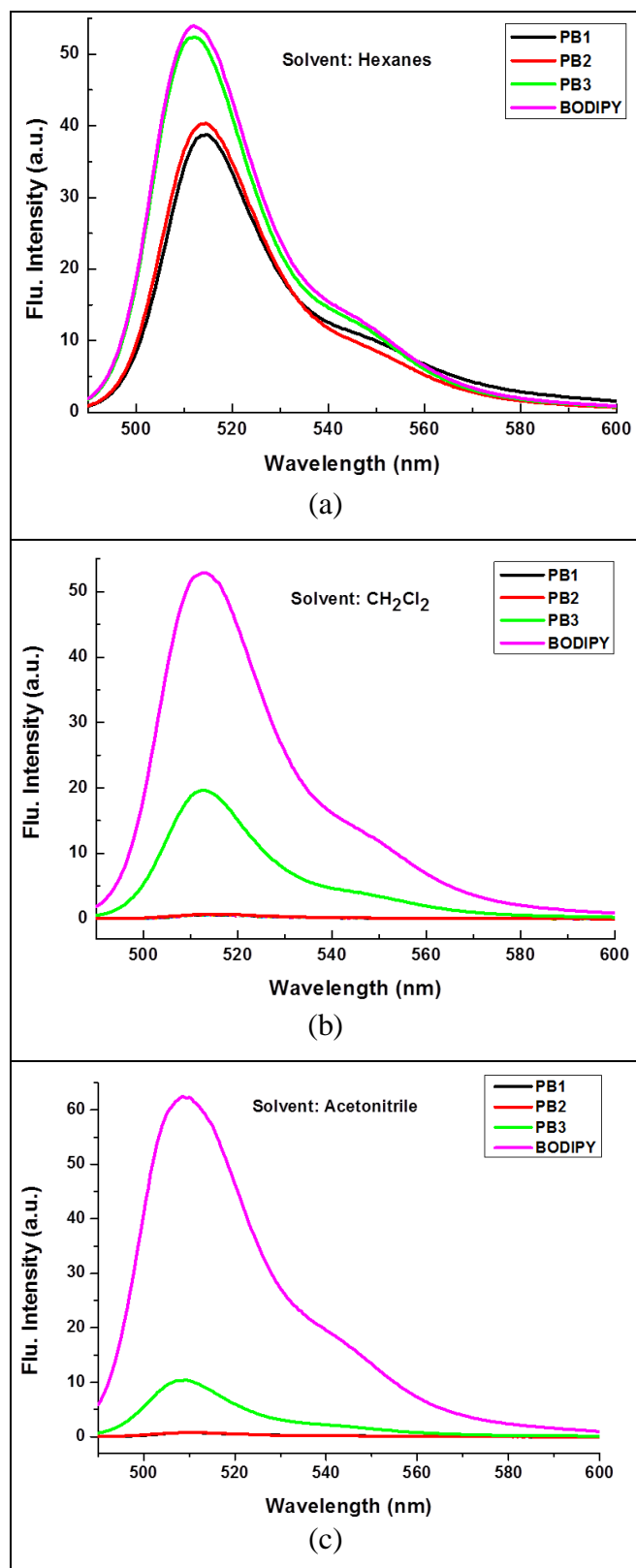
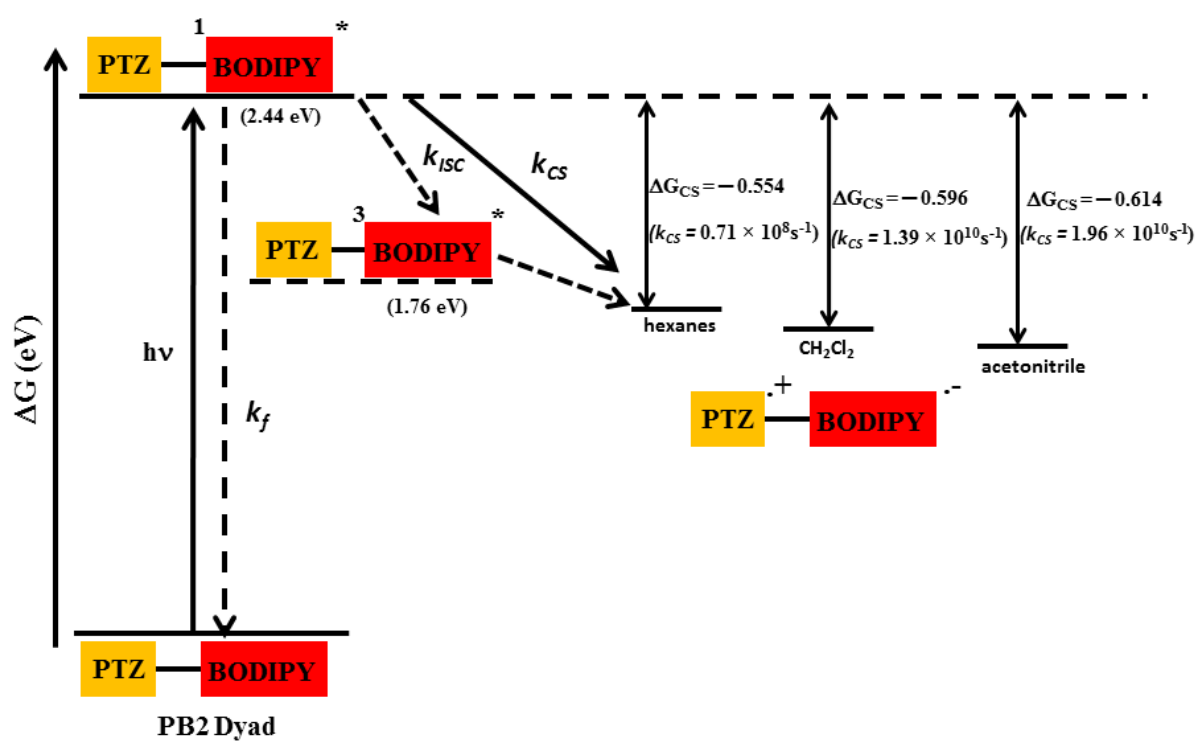
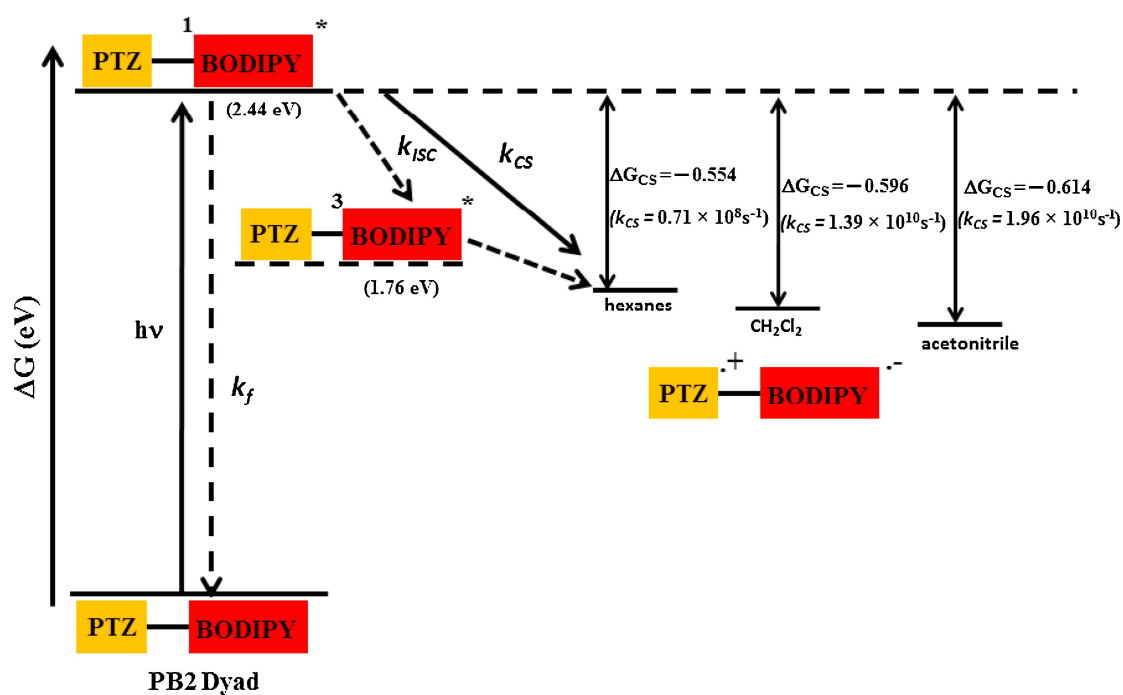


Figure 5

Figure 6





Graphical abstract

